Modeling and Analysis of Solid Axle Suspension and Its Impact on the Heavy Vehicles Stability

Gonzalo Guillermo Moreno Contreras
Department of Mechanical, Mechatronic and Industrial Engineering, Faculty of Engineering, University of Pamplona, Pamplona, 543050, Colombia

Rodrigo S Vieira
Department of Mechanical Engineering
Federal University of Santa Catarina – Florianopolis – Brazil

Daniel Martins
Department of Mechanical Engineering
Federal University of Santa Catarina – Florianopolis – Brazil

Abstract- The stability of heavy vehicles and the factors that can affect or improve it are studied. The leaf spring or rigid suspension is the oldest automotive suspension and continues to be a popularly used option for heavy vehicles. Although simple in appearance, this type of suspension causes many problems in modeling, due to the efforts and movements that occur. Taking these aspects into account, this paper presents a model of rigid suspension using mechanism theory and subsequent kinematic analysis using the Davies's method. This model is used to evaluate the influence of this type of suspension in the heavy vehicles stability. The proposed model is two-dimension, with two degrees-of-freedom, and allows relative motion between the sprung and unsprung masses of the vehicle, which is important in vehicle stability studies. This movement is detailed through a case study, in which the position of the vehicle's center of gravity changes due to the suspension's effect, affecting the vehicle's stability factor. This factor allows us to predict how stable a vehicle is when taking a curve and how its dynamic performance could be when making a determined route, which allows to improve road safety.

Keywords – Leaf spring, Suspension system, Kinematics, Davies method

I. INTRODUCTION

The stability of heavy vehicles has been the focus of research efforts for decades. The lateral vehicle stability can be evaluated through the static stability factor (*SSF*). This factor represents the maximum lateral acceleration - a_y (expressed in terms of gravity acceleration - g) in a quasi-static situation before one or more of the tires lose contact with the ground [1, 2, 3].

According to the classic vehicle stability analysis, the *SSF* factor is a function of the vehicle track width (t) and the height of the CG (h) (Eq. 1) [2].

$$SSF = \frac{a_y}{g} = \frac{t}{2h} \quad (1)$$

However, when a heavy vehicle is making a turn or an evasive maneuver, many characteristics of the vehicle, such as the suspension, tires, and chassis allow the vehicle body's inclination, changing the center of gravity's position and modifying the *SSF* factor.

Important researchers [1, 4, 5, 6] reported that the suspension system is one of the main factors influencing vehicle stability. Several models have been developed to represent the associated mechanism and its functioning during the rollover limit; however, such models do not take into account the change in the roll center height (CR) of the vehicle and the change in the lateral separation between the springs. In [7] defined the roll center as the point in the center of the axle, around which the body begins to roll when a lateral force acts.

This paper focuses on modeling a kinematic analysis of the suspension system under the action of a lateral inertial force. Mechanism theory is applied to model the tires and suspension systems, while the static analysis of the mechanism can be carried out using three concepts: screw theory, graph theory and the Davies's method [8, 9, 10, 11, 12] to describe the movement of the center of gravity (CG) and its roll center (CR).

The rest of the paper is organized as follows: in section 2, a mechanism representing a vehicle as a two-dimension model is developed; section 3, the static analysis of the vehicle stability using the proposed method is presented. The results presented in Section 3 are analyzed and discussed with a case study in section 4. Finally, conclusions are drawn in section 5.

II. Vehicle Model for Lateral Stability

There are several types of suspension systems, but the most commonly used by vehicles is the leaf spring [13], as shown in Fig. 1. For this analysis, only the rigid suspension system is taken into account. A two-dimensional vehicle model representing the last unit of a heavy vehicle (trailer) is developed below.

2.1 Suspension system -

The suspension system comprises the linkage between the sprung and unsprung masses of a vehicle, which reduces the movement of the sprung mass, allowing the tires to maintain contact with the ground, and filtering disturbances imposed by the ground [14].

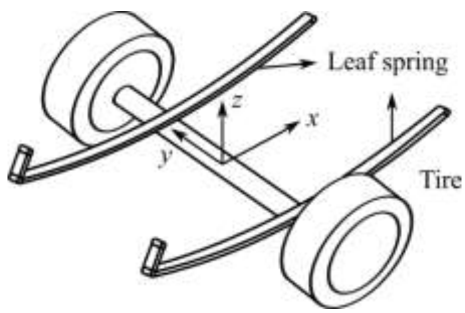

Figure 1. Solid axle with leaf spring [13].

The leaf spring is a mechanism that allows three motions of the vehicle body under the action of lateral forces, these are displacement in the *z*- and *y*-direction and a roll rotation about the *x*-axis [15, 16], as shown in Fig. 2(a).

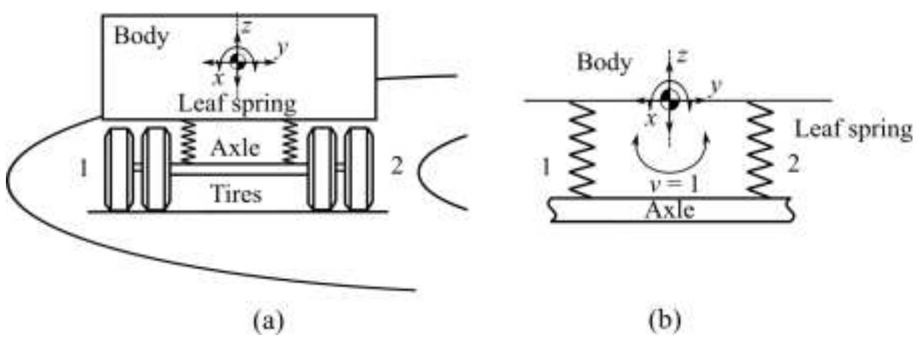

Figure 2. (a) Body motion. (b) Suspension system.

2.1.1 Kinematic chain of the suspension system

Mechanical systems can be represented by kinematic chains composed by links and joints, which facilities their modeling and analysis [17, 18, 19]. To model the kinematic chain Eq. (2) was used together with Eq. (3).

$$M = \lambda \times (n - j - 1) + j \quad (2)$$

$$v = j - n - 1 \quad (3)$$

where M is the degrees of freedom (DoF) or mobility of a mechanism, λ is the degrees of freedom of the space in which the mechanism is intended to function, n is the number of mechanism link, including the fixed link, j is the number of mechanism joints, and v is the number of independent loops in the mechanism.

The kinematic chain of the suspension system in Fig. 2(b), has 3-DoF ($M= 3$), the workspace is planar ($\lambda = 3$), and the number of independent loops is one ($v = 1$). Based on Eqs. (2) and (3) the kinematic chain of the suspension system should be composed of six links ($n = 6$) and six joints ($j = 6$).

To model this system, the following consideration is taken into account: leaf springs are assumed as compression springs and can be represented by prismatic joints "*P*" supported in revolute joints "*R*" [10, 20]. Applying these concepts to the suspension system's kinematic chain, a model with the configuration shown in Fig. 3(b) is proposed.

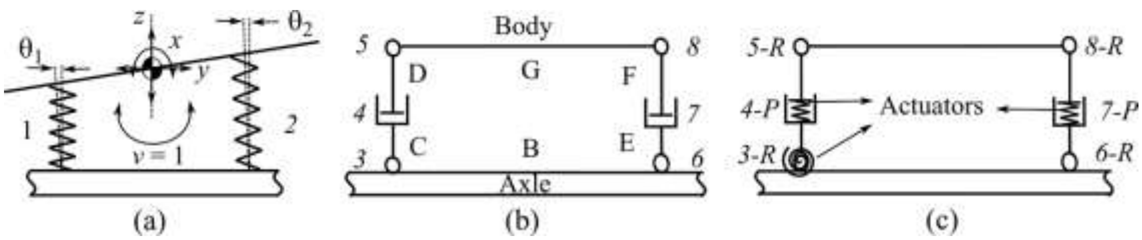

Figure 3. (a) Movement of the suspension system. (b) Kinematic chain of the suspension system. (c) Suspension system including actuators.

The kinematic chain of the suspension system is composed of six links identified by the letters B (vehicle axle), C and D (spring 1), E and F (spring 2) and G (the vehicle body); and six joints identified by numbers as follow: four revolute joints "R" (3,5, 6 and 8) and two prismatic joints "P" that represent the leaf springs of the system (4 and 7), as shown in Fig. 3(b and c).

The mechanism of Fig. 3(b) has 3-DoF, and requires three actuators to control its movement. The mechanism has one passive actuator in each prismatic joint (suspension system), and one passive actuator in the joint 3 (torsion spring), which controls the movement along the *x*- *y*- and *z*- axes, as shown in Fig. 3(c).

2.1.2 Kinematics of the suspension system

Given the pose (position and orientation) of the tires system, the kinematic problem consists of finding the corresponding rotation angle or displacement of all joints (active and passive) to achieve this position [21].

The movement of the tires is orientated by the forces acting on the mechanism (vehicle weight (W) and the inertial force (ma_y)). These forces affect the passive actuators of the mechanism, as shown in Fig. 4.

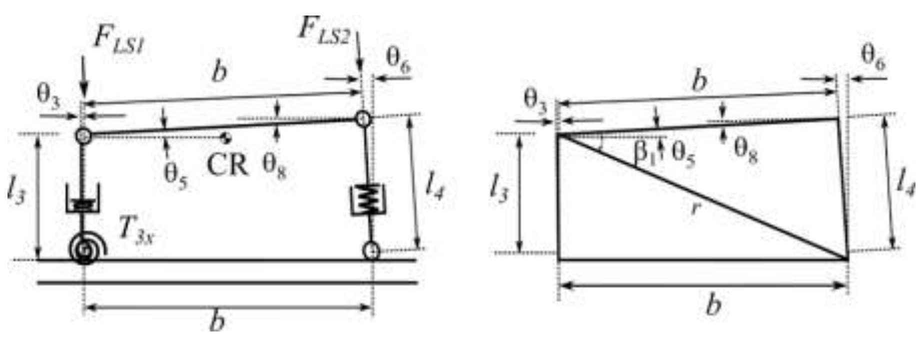

Figure 4. Movement of the suspension system.

Equations (4) to (10) define the kinematics of the suspension system.

$$\theta_3 = T_{3x} / k_{ts} \quad (4)$$

$$l_{3,4} = \delta_s + l_s = \frac{3Fl^3}{8ENBT^3} + l_s \approx \frac{-F_{LS1,2} + (W/2)}{k_s} + l_s \quad (5)$$

$$r = \sqrt{l_3^2 + b^2 - 2lb\cos\left(\tfrac{\pi}{2} + \theta_3\right)} \quad (6)$$

$$\beta_1 = \arccos\left(\left(b^2 + r^2 - l_4^2\right)/(2br)\right) \quad (7)$$

$$\theta_5 = \beta_1 + a\sin\left(\frac{b}{r}\sin\left(\tfrac{\pi}{2} + \theta_3\right)\right) - \frac{\pi}{2} \quad (8)$$

$$\theta_6 = \theta_3 + a\sin\left(\frac{b}{r}\sin\left(\tfrac{\pi}{2} + \theta_3\right)\right) - a\sin\left(\frac{b}{l_4}\sin(\beta_1)\right) \quad (9)$$

$$\theta_8 = \frac{\pi}{2} - \beta_1 - a\sin\left(\frac{b}{l_4}\sin(\beta_1)\right) \quad (10)$$

where T_{3x} is the momentum around the x-axis on the joint 3, k_{ts} is the spring's torsion coefficient, δ_S is the vertical deformation of the leaf spring [22], F is the static force on the leaf spring, l is the length of the leaf spring, N is the number of leaf, B is the width of the leaf, T is the thickness of the leaf, E is the modulus of elasticity of a multiple leaf, $F_{LS1;2}$ are the normal forces of the spring, W is the vehicle weight, l_S is the initial suspension height, k_S is the equivalent vertical spring stiffness of the leaf spring, $l_{3;4}$ are the instantaneous height of the spring, b is the lateral separation between the springs; and $\theta_{3,5,6,8}$ are the rotation angles of the revolute joints 3, 5, 6 and 8 respectively.

2.2 Vehicle model

Considering the model developed in our previous research [11], a two-dimensional vehicle model, which integrates the vehicle body, the suspension system, and the tires was developed (Fig. 5(a)). The kinematic chain of the vehicle model is composed of seven links identified by the letters A (road), B (vehicle axle and tires), C and D (spring 1), E and F (spring 2) and G (the vehicle body); and eight joints identified by numbers as follow: one revolute joint "R" (1 – tire-road contact - outer tire in the turn - Fig. 2(a)), four revolute joints "R" (3, 5, 6 and 8), two prismatic joints "P" that represent the leaf springs of the system (4 and 7), and one prismatic joint "P" (2 – tire-road contact - the lateral slide of the inner tire in the turn 2 - Fig. 2(a)), the workspace is planar (λ = 3); the proposed model has the parameters shown in the Figs. 5(b and c).

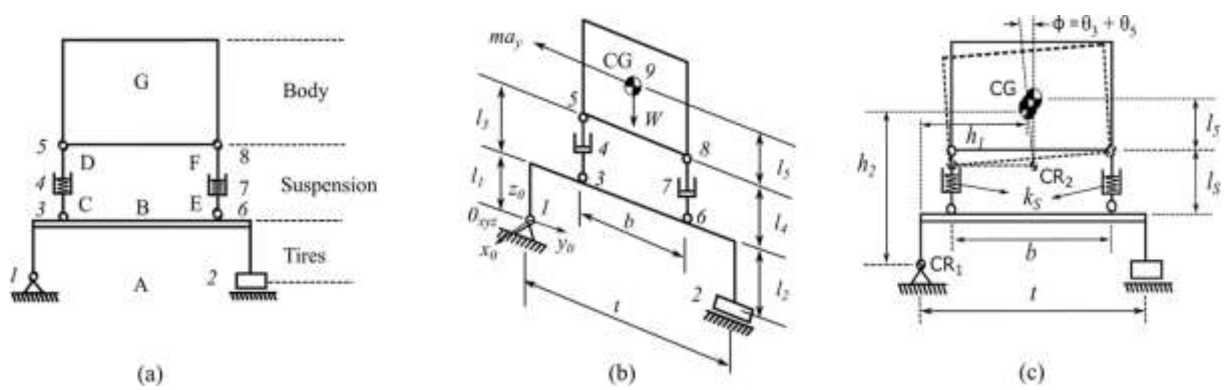

Figure 5. Vehicle model.

where t is the vehicle track width, b is the lateral separation between the springs, l_1 and l_2 are the dynamic rolling radius of the tires, l_5 is the CG height above the chassis, h_1 is the instantaneous lateral distance between the zero-reference frame and the CG, and h_2 is the instantaneous CG height, and l_S is the initial suspension height.

III. Static Analysis of Mechanism

Several methodologies allow us to obtain a complete static analysis of the mechanism; however, in this paper, the formalism described in [23] is used as the primary mathematical tool to analyze the mechanisms statically. Davies's method appears in published literature several times, and further details regarding its use can be found in [8, 9, 10, 11, 23, 24]. Davies's method was selected since it allows the static model for the mechanism to be obtained in a straightforward manner, and it is also easily adaptable to this approach.

Davies's method is a mathematical tool that uses screw theory and graph theory, together with Kirchhoff laws, to build and solve the static and kinematic analysis of any mechanism. Davies's method for static analysis can be described in a simplified way through the following steps:

1. Draw the kinematic chain of any given mechanism, identifying all of its "n" links, "f" external forces, and "e" direct couplings.

2. Draw the direct coupling graph "GA" for the mechanism with the links as the graph's vertices, and the joints, and its external forces as the edges of the graph. Assign positive directions to each edge with an arrow pointing from the minor to the major vertex.

3. Take note of the incidence matrix of the direct coupling graph $[I]_{n,e+f}$.

4. Generate the cut-set matrix $[Q]_{k;e+f}$ from the $[I]_{n,e+f}$ using the Gauss-Jordan elimination method. Where the number of cuts is defined ($k = n - 1$) (Identity matrix), and chords ($l = e + f - n + 1$) in the action graph and depict them.

5. Take note to the expanded cut-set matrix $[Q]_{k;c}$, where c is the number of constraints on the joints and external forces applied on the mechanism.

6. Write a wrench $\$_{J\lambda;c}$ for each constraint or external force on the mechanism, as follows:

$$\$_{J_{\lambda;c}} = \begin{bmatrix} -z \\ 1 \\ 0 \end{bmatrix} J_{F_y} + \begin{bmatrix} y \\ 0 \\ 1 \end{bmatrix} J_{F_z} + \begin{bmatrix} 1 \\ 0 \\ 0 \end{bmatrix} J_{M_x} \tag{11}$$

where λ is the degrees of freedom of the space in which the mechanism is intended to function.

7. Replace each wrench $\$_{J\lambda;c}$ in the expanded cut-set matrix $[Q]_{k;c}$ to obtain the generalized action matrix $[A_N]_{\lambda k;c}$.

8. Operate algebraically the generalized action matrix $[A_N]_{\lambda k;c}$ to statically solve the system.

The proposed model (Fig. 5) represents a vehicle making a planar curve, to simplify the model, the following considerations are taken into account:

- The analysis model is made in a steady-state in the x-direction;
- the model does not take into account disturbances imposed by the road, and the friction forces (tire-ground contact);
- the only external forces included were: the vehicle weight (W), the inertial force acting on the mechanism ($m\ a_y$), the normal forces of the springs ($F_{LS1;2}$), and T_{3x} is the momentum around the x-axis on the joint 6.

Using this method, the static of the mechanism can be defined, as exemplified in Eq. (12):

$$\left[\hat{A}_n\right]_{18\times 20}\left[\Psi\right]^T_{20\times 1} = \left[0\right]_{18\times 1} \tag{12}$$

where $[\hat{A}n]$ is the network unit action matrix, and $[\Psi]$ is the action vector of the mechanism's magnitudes.

It is necessary to identify the set of primary variables $[\Psi_p]$ (known variables), among the variables of Ψ, starting from the system (Eq. 12). Once identified, the system is divided into two sets, as shown by Eq. (13).

$$\left[\hat{A}_{ns}\right]_{18\times18}\left[\Psi_s\right]^T_{18\times1}+\left[\hat{A}_{np}\right]_{18\times2}\left[\Psi_p\right]^T_{2\times1}=\left[0\right]_{18\times1} \tag{13}$$

where $[\Psi_p]$ is the primary variable vector, $[\Psi_s]$ is the second variable vector (unknown variables), $[\hat{A}_{np}]$ are the columns corresponding to the primary variables and $[\hat{A}_{ns}]$ are the columns corresponding to the secondary variables. In this case, the primary variable vector and the secondary variable vector are shown in Eq. (14).

$$\begin{aligned}&\left[\Psi_p\right]^T_{2\times1}=\left[W \quad ma_y\right]^T\\&\left[\Psi_s\right]^T_{18\times1}=\left[F_{1y} \quad F_{3y} \quad F_{3z} \quad M_{4x} \quad F_{4n} \quad \cdots \quad T_{3x} \quad F_{LS1} \quad F_{LS2} \quad F_{1z} \quad F_{2z}\right]^T\end{aligned} \tag{14}$$

where F (forces) and M (momentum) denote the constraints on the mechanism joints (unknown variables), and W (vehicle weight) and ma_y (inertial force) are the known variables

Solving the system in Eq. (13), using the Gauss-Jordan elimination method, all secondary variables are functions of the primary variables (vehicle weight (W) and the inertial force (ma_y)). This analysis only considers the forces acting on the suspension and the tires; the last five rows of solution system provide the next equations:

$$T_{3x}+c_1\times W+c_2\times ma_y=0 \tag{15}$$

$$F_{LS1}+c_3\times W+c_4\times ma_y=0 \tag{16}$$

$$F_{LS2}+c_5\times W+c_6\times ma_y=0 \tag{17}$$

$$F_{1z}+\left(\left(h_1-t\right)/t\right)\times W-\left(h_2/t\right)\times ma_y=0 \tag{18}$$

$$F_{2z}-\left(h_1/t\right)\times W+\left(h_2/t\right)\times ma_y=0 \tag{19}$$

where c_i are constants of the equation system solution.

At the rollover limit condition, the normal load, F_{2z}, reaches zero and on applying this in the Eq. (19), the *SSF* factor can be calculated as:

$$SSF=\frac{a_y}{g}=\frac{h_1}{h_2} \tag{20}$$

Making a comparison between the Eq. (1) and Eq. (20); it is demonstrated that the *SSF* factor is dependent on the lateral and vertical location of the vehicle center of gravity (CG).

For calculating the *SSF* factor, the inertial force is increased until the lateral load transfer (*LLT*) in the axle is complete (all the load is transferred from the inner tire to the outer tire as the vehicle makes a turn) [11, 25]. From the Eqs. (15) to (19) the instantaneous forces acting on the mechanism can be obtained. These forces modify the configuration of the suspension system Eqs. (4) to (10).

IV. Case Study

For this analysis, a two-dimensional vehicle model that represent the last axle of the trailer is proposed. In this model, a suspension system with the tandem axle is used, and the suspension parameters are dependent on the construction materials. Harwood [26] indicated that the range of values for the vertical spring stiffness per axle is k_s = 1500-2400 kN.m^{-1}. Another important parameter is the dynamic rolling radius or loaded radius l_i, the model proposed considers Michelin® [27] radial tires with dynamic rolling radius l_i = 0:499 m. Figure 6 and Table 1 show the heavy vehicle parameters used in this analysis [28].

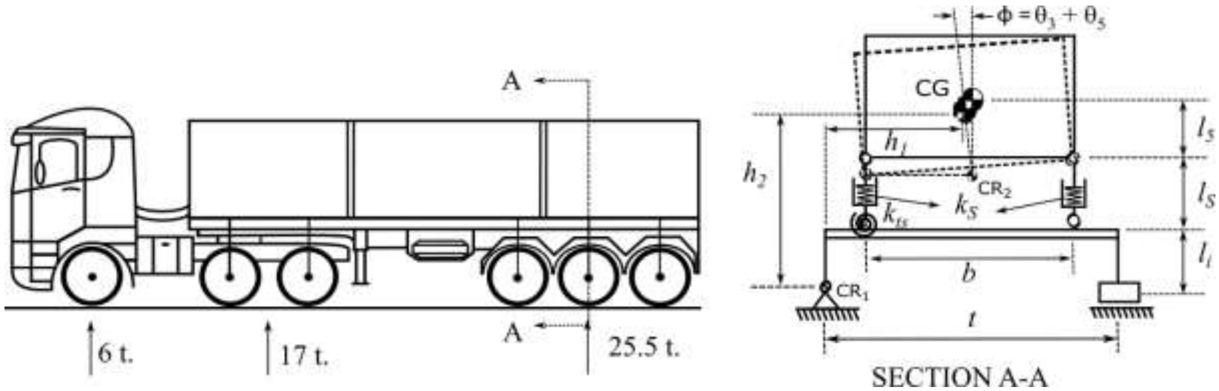

Figure 6. Parameters of heavy vehicle.

Table 1. Parameters of heavy vehicle.

Parameter	Value	Units
Vehicle weight - W	250	kN
Track width -t	1.86	m
Equivalent vertical spring stiffness – $k_{s.equ}$.	5400	kN/m
Spring's torsion coefficient – k_{ts}	$k_{ts} >>> k_{s.equ.}$	kN/m
Initial suspension height - l_s	0.205	m
Dynamic rolling radius - l_i	0.499	m
Lateral separation between the springs - b	0.95	m
Height of CG above the chassis - l_5	1.346	m

The simulation model was made in MATLAB®, for the *SSF* factor calculation (Eq. (19) and (20)), the inertial force is increased until the entire lateral load transfer (*LLT*) was transferred from the inner to the outer tires, along with the turn [25].

In the analysis of the proposed model, a reduction of around 10% in the vehicle's *SSF* factor can be observed. This reduction results from the suspension system's action, which allows a body roll angle of $\phi = \theta_3 + \theta_5 = 3.87^0$, as shown in Fig. 7.

Furthermore, this model allows the determination of the vertical (h_2 - the instant CG height – shown in Fig. 8) and lateral (h_1 - the instant lateral distance between the zero-reference frame and the center of gravity - shown in Fig. 9) movements of the vehicle's center of gravity (CG).

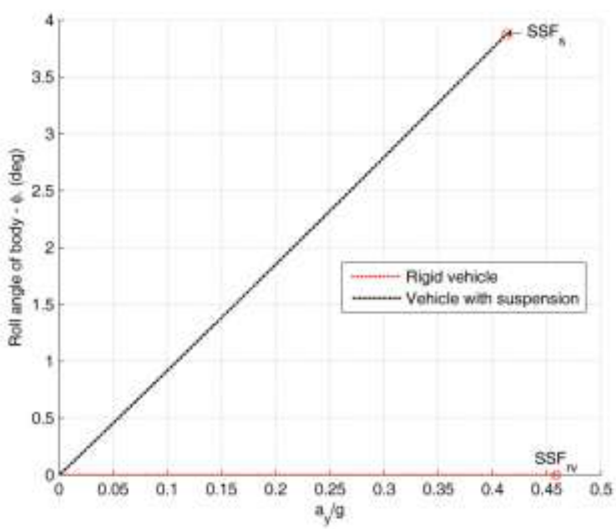

Figure 7. The roll angle of the vehicle model.

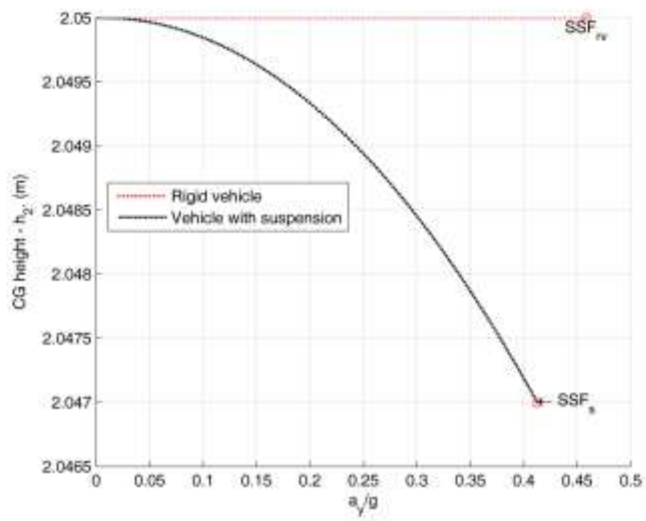

Figure 8. The instant CG height (h_2).

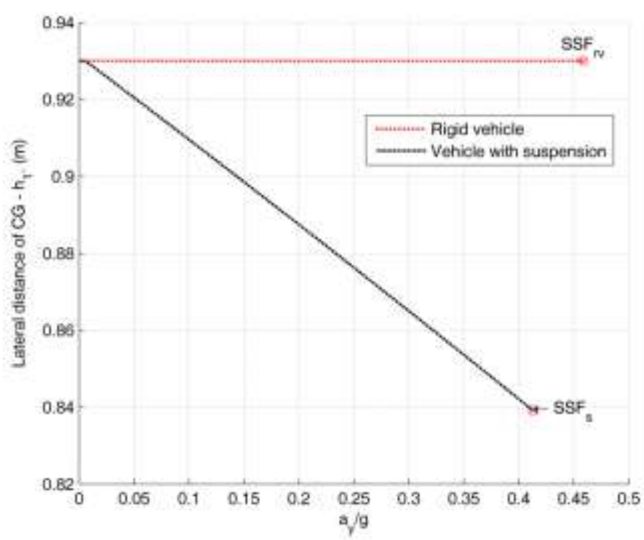

Figure 9. The instant lateral distance between the zero-reference frame and the center of gravity (h_1).

In the Fig 10 can be observed the vertical movement of the vehicle's roll center (CR)(Fig. 6 – SECTION A-A); for the rigid vehicle model, all vehicle rotates around the joint 1 (CR_1: $h=0$); and for the vehicle model with the suspension system, the CR is located in the instant center of rotation of the vehicle body (CR_2: $h = l_1 + l_3 \cos(\theta_3)$)

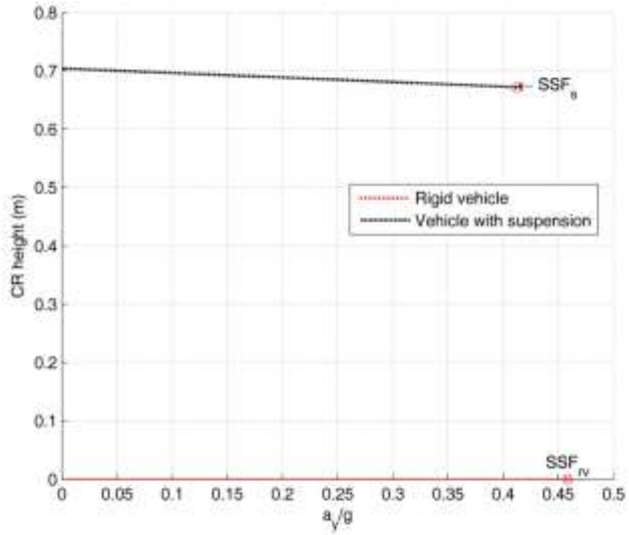

Figure 10. Instantaneous CR heights.

Finally, the proposed model shows how the change of *b* (lateral separation between the springs) influences the *SSF* factor. Some heavy vehicles with tanker semi-trailer have a more lateral separation between the springs; this causes a decrease in its roll angle, and therefore increases its *SSF* factor by one centimeter of lateral separation between the springs. This is deu to the gain of stability around 0.001 g. as shown in Fig. 11.

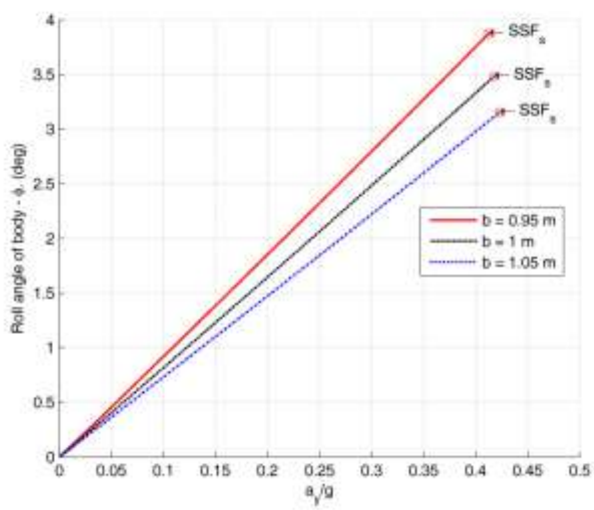

Figure 11. Figure 11. Change of *b* - *SSF* factor.

V. CONCLUSIONS

The proposed suspension system allows the determination of its influence on the calculation of the *SSF* factor of the vehicle and the changes in the position of its center of gravity (CG) and roll center (CR).

This model also shows how the change in the lateral separation between the springs (*b*) is an important factor to consider in the design and construction of vehicles, as more lateral separation will increase vehicle stability.

The decrease in the *SSF* factor is significant; since it allows new road speed limits to be determined, aiming to improve road safety and decreasing the occurrence of accidents related to vehicle stability.

ACKNOWLEDGEMENTS

This research was supported by the Brazilian governamental agencies Coordenação de Aperfeiçoamento de Pessoal de Nível Superior (CAPES) and Conselho Nacional de Desenvolvimento Cientifico e Tecnológico (CNPq).

REFERENCES

[1] Winkler, C. B., Experimental determination of the rollover threshold of four tractor-semitrailer combination vehicles. Final report. 1987.

[2] Gillespie, T. D., Fundamentals of vehicle dynamics. Vol. 400. Warrendale, PA: Society of automotive engineers, 1992.

[3] Hac, A., Rollover stability index including effects of suspension design. SAE Transactions, 2002, 1403-1413.

[4] Winkler, C B., Rollover of heavy commercial vehicles, SAE, Warrendale, 1999.

[5] Chang, T., Effect of vehicles' suspension on highway horizontal curve design. Journal of transportation engineering, Vol. 127(1), 2001, 89-91.

[6] Miege, A. J. P. and Cebon, D., Active roll control of an experimental articulated vehicle. Proceedings of the Institution of Mechanical Engineers, Part D: Journal of Automobile Engineering, Vol. 219(6), 2005, 791-806.

[7] Reimpell, J., Stoll, H., and Betzler, J., The automotive chassis: engineering principles. Elsevier, 2001.

[8] Tsai, L. W., The mechanics of Serial and Parallel manipulators. Robot Analysis, John Wiley & Sons, Inc, 1999.

[9] Davies, T. H., The 1887 committee meets again. Subject: freedom and constraint. 2000.

[10] Erthal, J., Modelo cinestático para analise de rolagem em veículos. Ph.D. Thesis, Federal University of Santa Catarina, Florianópolis, Brazil. 2010.

[11] Moreno, G.G., Nicolazzi, L., Vieira, R., Martins, D., Three-dimensional analysis of the rollover risk of heavy vehicles using Davies method, 14th World Congress in Mechanical and Machine Science (IFToMM2015), Taipei-Taiwan, Vol. 10, 2015. DOI10.6567/IFToMM.14TH.WC.PS4.006.

[12] Moreno, G., Nicolazzi, L., Vieira, R. S., and Martins, D., Suspension and tyres: the stability of heavy vehicles, International Journal of Heavy Vehicle Systems, Vol. 24 (4), 2017, 305-326. doi:10.1504/IJHVS.2017.10007635.

[13] Rill, G., Kessing, N., Lange, O., and Meier, J., Leaf spring modelling for real time applications. 18th IAVSD-Symposium in Atsugi-Japan, Vol. 3, 2003, 1-22.

[14] Ledesma, R., and Shin S., Heavy and medium duty vehicle suspension-related performance issues and effective analytical models for system design guide. No. 1999-01-3781. SAE Technical Paper, 1999.

[15] Rempel, M.R., Improving the dynamic performance of multiply-articulated vehicles., Master's thesis, The University of British Columbia, Vancouver, Canada. 2001.

[16] Jazar, R., Vehicle Dynamics - Theory and Application. 2nd Edition, Springer, ISBN 978-0387742441, 2009.

[17] Kutzbach, K., Mechanische leitungsverzweigung, Maschinenbau Vol. 8 (21), 1929, 710-716.

[18] Crossley, F.R.E. A contribution to Grübler's theory in number synthesis of plane mechanisms. ASME Journal of Engineering Industry, 1964, 1-8.

[19] Tsai, L.W., Mechanism Design: Enumeration of Kinematic Structures According to Function. CRC Press., ISBN 0849309018, 2001.

[20] Lee, U., A Study on a Method for Predicting the Vehicle Controllability and Stability Using the Screw Axis Theory, PhD. These. Hanyang University, Seoul, South Korea. 2001.

[21] Mejia, L., Simas, H., Martins, D., Force capability maximization of a 3RRR symmetric parallel manipulator by topology optimization., 22nd International Congress of Mechanical Engineering (COBEM 2013). 2013.

[22] Dhoshi, N., Ingole, N., and Gulhane, U., Analysis and modification of leaf spring of tractor trailer using analytical and finite element method, International Journal of Modern Engineering Research, Vol.1(2), 2011, 719-722.

[23] Davies, T.H., Mechanical networks-III wrenches on circuit screws, Mechanism and Machine Theory Vol. 18(2), 1983, 107-112.

[24] Davies, T.H., Mechanical networks-I passivity and redundancy, Mechanism and Machine Theory Vol. 18(2), 1983, 95-101.

[25] Rill, G., Road Vehicle Dynamics: Fundamentals and Modeling. CRC Press, ISBN 978-1-4398-3898-3, 2011.

[26] Harwood, D. W., Torbic, D. J., Richard, K. R., Review of Truck Characteristics as Factors in Roadway Desing, National Cooperative Highway Research Program, ISBN 0-309-08779-1, 2003.

[27] Michelin, Michelin XZA Tire. 2013.

[28] Ervin, R.D., Guy, Y., The influence of weights and dimensions on the stability and control of heavy duty trucks in Canada, Tech. rep., UMTRI – The University of Michigan Transportation Research Institute, Final Report UMTRI-86-35/III. 1986.